Studies in Engineering and Exact Sciences
ISSN: 2764-0981

Low thickness effect on the properties of Mn-doped ZnO thin films synthesized by sol-gel spin coating technique

Efeito da baixa espessura nas propriedades de filmes finos de ZnO dopados com Mn sintetizados pela técnica de spin coating via sol-gel

Efecto del bajo espesor en las propiedades de películas delgadas de ZnO dopadas con Mn sintetizadas mediante la técnica de recubrimiento por centrifugación sol-gel

DOI: 10.54021/seesv5n2-443

Originals received: 10/04/2024
Acceptance for publication: 10/25/2024

Elhadj Benrezgua
Doctor in Physics
Institution: Laboratory of Materials and Renewable Energy, Department of Natural and Life Sciences, Faculty of Sciences, University of M'sila University Pole, Road Bourdj Bou Arreiridj, M'sila 28000 Algeria
Address: M'sila, Algeria
E-mail: elhadj.benrezgua@univ-msila.dz

Ammar Boukhari
Doctor in Physics
Institution: Laboratory of Materials and Renewable Energy, Department of Mechanical Engineering, Faculty of Technology, University of M'sila University Pole, Road Bourdj Bou Arreiridj, M'sila 28000 Algeria
Address: M'sila, Algeria
E-mail: Ammar.Boukhari@univ-msila.dz

Rabie Amari
Doctor in Physics
Institution: Laboratory of Materials and Renewable Energy, Department of Civil Engineering, Faculty of Technology, University of M'sila University Pole, Road Bourdj Bou Arreiridj, M'sila 28000, Algeria
Address: M'sila, Algeria
E-mail: Rabie.Amari@univ-msila.dz

Smail Terchi
Doctor in Chemistry
Institution: Laboratory of Materials and Renewable Energy, Department of Chemistry, Faculty of Sciences, University of M'sila University Pole, Road Bourdj Bou Arreiridj, M'sila 28000, Algeria
Address: M'sila, Algeria
E-mail: Smail.Terchi@univ-msila.dz

Djelel Kherifi
Doctor in Physics
Institution: Laboratory of Materials and Renewable Energy, Department of Physics, Faculty of Sciences, University of M'sila University Pole, Road Bourdj Bou Arreiridj, M'sila 28000, Algeria
Address: M'sila, Algeria
E-mail: djelel.kherifi@univ-msila.dz

Djamel Allali
Doctor in Physics
Institution: Laboratory of Materials and Renewable Energy, Department of Mechanical Engineering, Faculty of Technology, University of M'sila University Pole, Road Bourdj Bou Arreiridj, M'sila 28000, Algeria
Address: M'sila, Algeria
E-mail: Djamel.Allali@univ-msila.dz

Fathi Messaoudi
PhD Student in Physics
Institution: Laboratory of Materials Physics, Radiation and Nanostructures (LPMRN), Department of Physics, Faculty of Sciences, Mohamed El Bachir El Ibrahimi University, 34000 Bordj Bou-Arreridj, Algeria
Address: M'sila, Algeria
E-mail: fathi.messaoudi@univ-bba.dz

Bahri Deghfel
Doctor in Physics
Institution: Laboratory of Materials and Renewable Energy, Department of Physics, Faculty of Sciences, University of M'sila University Pole, Road Bourdj Bou Arreiridj, M'sila 28000, Algeria
Address: M'sila, Algeria
E-mail: Bahri.Deghfel@univ-msila.dz

ABSTRACT
In this study, 7% manganese-doped zinc oxide (MZO) thin films with varying low thicknesses were synthesized using the spin coating method. The structural, optical, and morphological properties of MZO films with different film thickness, were systematically investigated. The crystallite structure, superficial morphology, and optical characteristics were analyzed using X-ray diffraction (XRD), atomic force microscopy (AFM), scanning electron microscopy (SEM), and ultraviolet–visible spectroscopy (UV-Vis). Structural analysis confirmed that all films exhibit a hexagonal wurtzite phase with a pronounced peak along the c-axis, and slight variation in low thickness significantly affected the structural parameters. The surface morphology demonstrated good uniformity, characterized by rounded grain shapes in the plane, while surface roughness was found to be increased with increasing film thickness. Optical analysis revealed that as the number of coatings increased, both transmittance and band gap energy decreased, accompanied by a redshift in the absorption edge across all samples. This behavior is attributed to light scattering, as well as an increase in the refractive index and dielectric function with visible light energy, influenced by the number of layers and corresponding

crystallite size.

Keywords: MZO Thin Films. Low Thickness. Optical Properties. Spin Coating.

RESUMO

Neste estudo, filmes finos de óxido de zinco dopados com 7% de manganês (MZO) com espessuras reduzidas variadas foram sintetizados usando o método de spin coating. As propriedades estruturais, ópticas e morfológicas dos filmes de MZO com diferentes espessuras foram investigadas sistematicamente. A estrutura cristalina, a morfologia superficial e as características ópticas foram analisadas utilizando difração de raios X (XRD), microscopia de força atômica (AFM), microscopia eletrônica de varredura (SEM) e espectroscopia de ultravioleta-visível (UV-Vis). A análise estrutural confirmou que todos os filmes exibem uma fase hexagonal tipo wurtzita, com um pico pronunciado ao longo do eixo c, e pequenas variações na espessura afetaram significativamente os parâmetros estruturais. A morfologia da superfície demonstrou boa uniformidade, caracterizada por grãos arredondados no plano, enquanto a rugosidade da superfície aumentou com a espessura do filme. A análise óptica revelou que, com o aumento do número de camadas, tanto a transmitância quanto a energia de gap diminuíram, acompanhadas de um deslocamento para o vermelho na borda de absorção em todas as amostras. Esse comportamento é atribuído à dispersão de luz, bem como ao aumento do índice de refração e da função dielétrica com a energia da luz visível, influenciado pelo número de camadas e pelo tamanho dos cristalitos.

Palavras-chave: Filmes Finos de MZO. Baixa Espessura. Propriedades Ópticas. Spin Coating.

RESUMEN

En este estudio, se sintetizaron películas delgadas de óxido de zinc dopadas con 7% de manganeso (MZO) con diferentes espesores reducidos utilizando el método de recubrimiento por centrifugación. Se investigaron sistemáticamente las propiedades estructurales, ópticas y morfológicas de las películas de MZO con diferentes espesores. La estructura cristalina, la morfología superficial y las características ópticas se analizaron mediante difracción de rayos X (XRD), microscopía de fuerza atómica (AFM), microscopía electrónica de barrido (SEM) y espectroscopía ultravioleta-visible (UV-Vis). El análisis estructural confirmó que todas las películas exhiben una fase hexagonal tipo wurtzita con un pico pronunciado a lo largo del eje c, y una ligera variación en el espesor redujo significativamente los parámetros estructurales. La morfología superficial demostró buena uniformidad, caracterizada por formas de granos redondeados en el plano, mientras que se encontró que la rugosidad de la superficie aumentaba con el espesor de la película. El análisis óptico reveló que a medida que aumentaba el número de recubrimientos, tanto la transmitancia como la energía de banda prohibida disminuían, acompañadas de un corrimiento al rojo en el borde de absorción en todas las muestras. Este comportamiento se atribuye a la dispersión de la luz, así como a un aumento en el índice de refracción y la función dieléctrica con la energía de la luz visible, influenciado por el número de capas y el tamaño correspondiente de los cristalitos.

Palabras clave: Películas Delgadas de MZO. Bajo Espesor. Propiedades Ópticas. Recubrimiento por Centrifugación.

1 INTRODUCTION

Zinc oxide (ZnO) is a II-VI semiconductor characterized by an exciton binding energy of 60 meV and a wide direct band gap (3.37eV) at room temperature. These properties, combined with its high chemical stability, non-toxicity, low growth temperature, and transparency in the visible spectrum, position ZnO as a promising material for various applications. ZnO has potential uses in devices such as transparent electrodes (You, Tu et al. 2012), gas sensors (Zhu and Zeng 2017), solar cells (Giannouli and Spiliopoulou 2012), spintronic devices (Rajamanickam, Rajashabala et al. 2014), and UV light-emitting diodes (LEDs) (Pearton and Ren 2014). Numerous methods for fabricating ZnO thin films were explored, including pulsed laser deposition (Smaali, Abdelli-Messaci et al. 2020), RF magnetron sputtering (Bouznit, Beggah et al. 2012), molecular beam epitaxy (MBE) (Kato, Sano et al. 2003), spray pyrolysis (Gaikwad, Jagdale et al. 2014), and chemical vapor deposition (CVD) (Müller, Huber et al. 2019). The sol-gel method, in particular, has gained interest for its simplicity, cost-effectiveness (Baig and Butt 2023, Bouderbala, Guessoum et al. 2024), and benefits like large-area deposition and uniform film thickness (Chen, Wang et al. 2007). The effect of film thickness on ZnO's properties has been extensively studied using these physical and chemical synthesis methods, further enhancing its potential for diverse device applications(Kakati, Jee et al. 2010, Mortezaali, Taheri et al. 2016, Namoune, Touam et al. 2017, Pal, Singhal et al. 2017, Kumar, Singh et al. 2019).

In recent years, extensive research has been dedicated to improving the properties of ZnO through doping with elements such as Co, Mn, Al, and Mg (Chen, Wang et al. 2007). Manganese (Mn) has been extensively studied as a dopant, particularly in ZnO thin films, where various physical properties have been explored under different experimental conditions (Xin, Hu et al. 2014). This research is driven by ZnO's potential for optoelectronic applications in the ultraviolet and blue spectral ranges (Shishiyanu, Shishiyanu et al. 2005), as well as its unique characteristics as a dilute magnetic semiconductor (DMS). Notably,

the properties of MZO thin films are strongly influenced by film thickness. Studies on films deposited using RF magnetron sputtering show that increasing thickness enhances crystallinity and grain size, while reducing strain, band gap energy, and average transmittance. These films typically crystallize in the wurtzite phase with a preferred (002) c-axis orientation(Rajalakshmi and Angappane 2014, Venkaiah and Singh 2014, Kayani, Nazir et al. 2015).

This study aims to experimentally investigate the effect of low thickness on the properties of MZO thin films. The films were elaborated using the sol-gel spin coating method and deposited on glass substrates, which offers several advantages, including producing homogeneous films with uniform thickness, enabling large-area deposition at low temperatures, and facilitating easy composition control. Using various analytical techniques, a comprehensive analysis will be conducted to evaluate the morphological, structural, and optical characteristics of the MZO thin films.

2 EXPERIMENTAL DETAIL

The sol-gel spin coating technique was employed to fabricate MZO thin films on glass substrates. The solution was prepared by dissolving Zn acetate dihydrate [$Zn(CH_3COO)_2 \cdot 2H_2O$] and Mn acetate tetrahydrate [$Mn(CH_3COO)_2 \cdot 4H_2O$] at a 7% molar concentration in isopropanol [$(CH_3)_2CHOH$], with monoethanolamine [$NH_2CH_2CH_2OH$] added as a stabilizer, maintaining a 1:1 molar ratio between the stabilizer and metal ions. The obtained solution was stirred at 65 °C for 1 hour and allowed to age at room temperature for 24 hours, and then deposited onto clean glass substrates using a spin rate of 2000 rpm for 30 seconds, followed by drying. The substrates were pre-cleaned in an ultrasonic bath with ethanol, acetone, and deionized water for 10 minutes prior to deposition. To remove solvents and organic residues, the samples were preheated at 250 °C for 5 minutes. The preheating and coating processes were repeated to achieve the desired thickness, after which the samples were annealed at 500 °C for 1 hour.

The film thickness was determined using a Stylus Profilometer (model D 500). The structural properties were characterized with an X-ray diffractometer (XRD; X'Pert PRO MPD) employing Cu-Kα radiation, which has a wavelength of λ

= 1.5406 Å. The surface of samples was analyzed using AFM (Asylum Research, MFP-3D Classic) and FESEM (Zeiss Supra 35 VP). The optical transmission were recorded using an UV–vis spectrophotometer (UV-3101 PC-Shimadzu) over the range of 350–800 nm, allowing for the evaluation of the bandgap.

3 RESULTS AND DISCUSSION

The structural properties of MZO thin films were investigated using XRD, revealing three dominant peaks: (100), (002), and (101), indicating the polycrystalline phase of the samples with a preferential orientation along the c-axis (Figure 1). No secondary phases such as $ZnMnO_3$ or Mn_3O_4 were detected (Fabbiyola, Kennedy et al. 2016, Kayani, Zulfiqar et al. 2019), and the wurtzite phase remained unchanged after the incorporation of Mn^{2+} into the ZnO structure (Yang and Zhang 2013). The (002) peak was notably more intense than the others, suggesting the preferential growth along the c-axis (Figure 1.a), which is attributed to the surface free energy stability of the (002) planes(Xin, Hu et al. 2014). The lattice constants c slightly increased from 5.220 Å (1 layer) to 5.282 Å (5 layers). All values were found to be lower than the bulk ZnO value of 5.207 Å (JCPDS 36–1451), and the (002) peak position shifted towards higher angles as the coating number increased (Table 1).

Figure 1. (a) XRD patterns, (b) Variation of strain, (c) Variation of crystallite size, (d) Variation of FWHM and (e) Variation of $TC_{(hkl)}$ of MZO samples for various coating number.

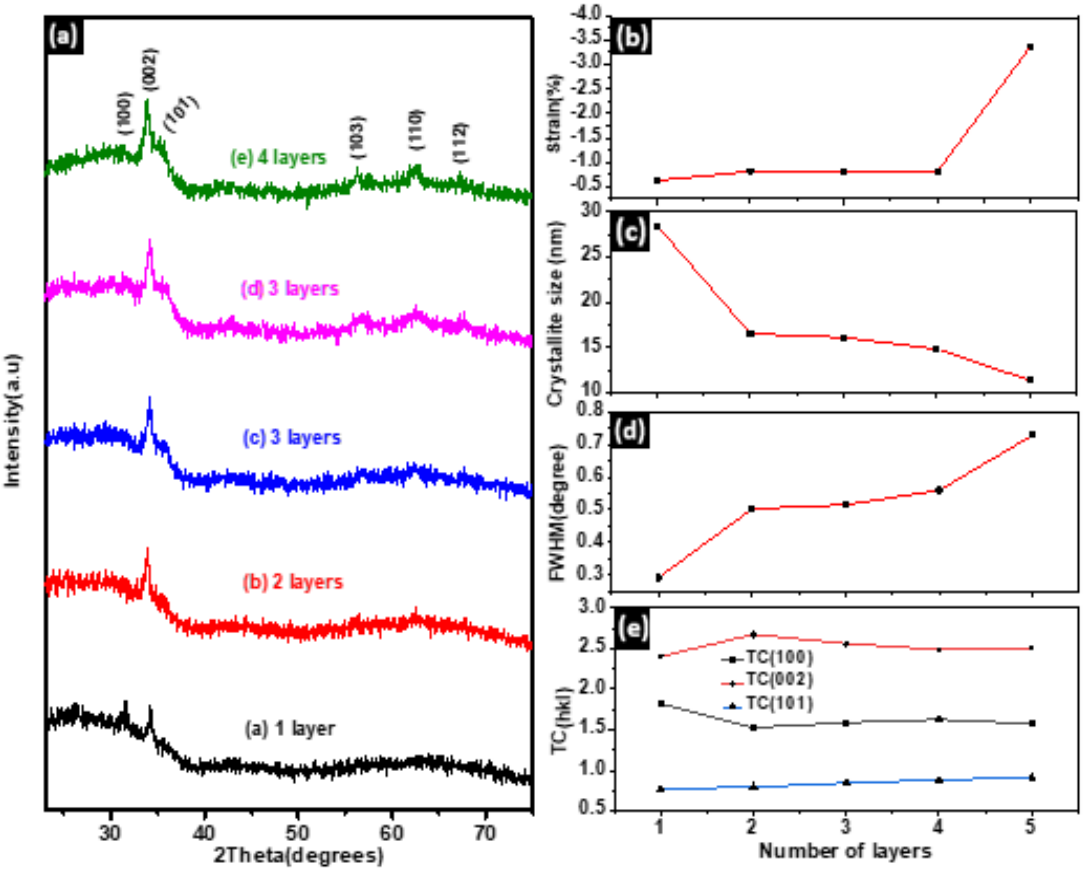

Source: self-authored

The lattice strain (ε) and the average crystallite size (D) are estimated using the procedure indicated in Ref. (Amari, Mahroug et al. 2018). The strain value increases with film thicknesses (Figure 2.b), indicating the films become stressed due to the substitution of Zn^{2+} by Mn^{2+} cations. The D, estimated from the full width at half maximum (FWHM) of the (002) peak (Figure 2.b.c), increases from 26.45 nm for a 1 layer to 69.39 nm for 5 layers (Table 1). Similar trend was reported in the literature (Venkaiah and Singh 2014, Kayani, Nazir et al. 2015).

The texture coefficient, $TC_{(hkl)}$, for all observed peaks in the XRD patterns of MZO samples was determined at different thicknesses (Figure 1.e). The (002) plane exhibits the highest TC(hkl) value, signifying a preferred growth orientation along the c-axis, regardless of the coating number (Boukhari, Deghfel et al. 2021).The degree of c-axis orientation varies with the coating number, where a higher $TC_{(hkl)}$ reflecting improved crystallinity(Boukhari, Deghfel et al. 2021) . The intensity of the (002) diffraction peak increases with film growth, reaching a maximum at 5 layers. Beyond this point, the (002) peak intensity continues to

increase in MZO thin film. The intensity of the (100) and (101) peaks was observed to be increased with the coating number for MZO samples. However, the $TC_{(hkl)}$ values for the primary (002) peak in MZO samples show slight variations, ranging from 2.40 to 2.67, depending on the coating number (Boukhari, Deghfel et al. 2021, Boukhari, Deghfel et al. 2021).

Table 1. Morphological and structural parameters of 7%MZO samples for various coating numbers.

Coating number	Thickness [nm]	2θ (°)	c (Å)	FWHM (°)	Peak intensity	Crystallite size (nm)	Grain size (AFM) (nm)	Strain (%)	Rrms (nm)
1	99	34.178	5.220	0.292	(002)	28.47	26.45	-0.699	20.40
2	291	34.238	5.225	0.502	(002)	16.54	24.66	-0.813	20.26
3	437	34.177	5.224	0.515	(002)	16.13	38.07	-0.801	32.12
4	577	34.187	5.225	0.559	(002)	14.85	42.23	-0.820	33.60
5	681	33.860	5.282	0.728	(002)	11.41	69.39	-3.378	56.62

Source: self-authored

The surface morphology of the samples was investigated by AFM (Figure 2; 2D and 3D images) and FESEM (Figure 3). Surface roughness and grain size were estimated using WsXM software from the AFM images (Horcas, Fernández et al. 2007). All films exhibited uniform growth, with grains having a round shape in the plane, and their size generally increased with the number of coatings. This indicates that grain growth is predominantly vertical initially and then becomes lateral as film thickness increases, which correlates with our XRD results. The MZO samples display columnar grains growing along the (002) direction. The surface roughness of the samples also increased with thickness, while the surface became smoother at lower coating numbers, consistent with the average grain size values (Table 1) and previous findings reported in the literature(Boukhari, Deghfel et al. 2021, Boukhari, Deghfel et al. 2021).

Figure 2. 1.0 X 1.0 μm^2 2D and 3D AFM images of MZO samples: (a) 1 coating, (b) 2 coatings, (c) 3 coatings, (d) 4 coatings, (e) 5 coatings.

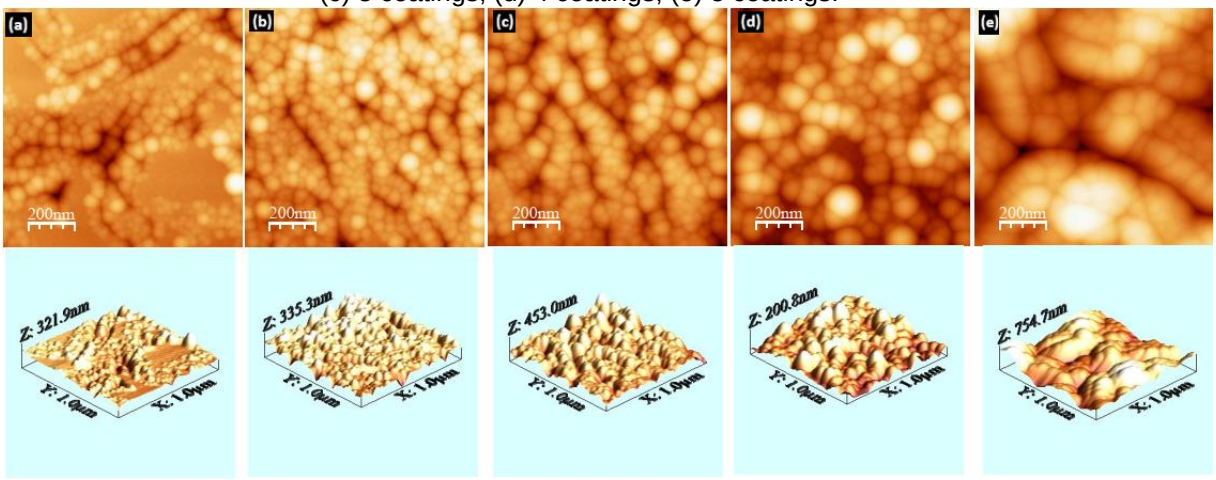

Source: self-authored

Figure 3 displays the FESEM 2D images and their corresponding cross-sectional images at a magnification of 20,000× of MZO samples for various coating numbers. The images reveal a morphology characterized by irregularly sized aggregated clusters. The film thicknesses, estimated from the cross-sectional images, ranged from approximately 99 to 688 nm (inset in Figure 3), varying with the number of deposition layers: 99 nm for 1 layer, 291 nm for 2 layers, 447 nm for 3 layers, 577 nm for 4 layers, and 681 nm for 5 layers. Naturally, the film thickness increases with the coating number (Table 1). The average thickness for each layer was determined to be 139 nm.

Figure 3. FESEM 2D images and the cross-sectional images of MZO samples: (a) 1 coating, (b) 2 coatings, (c) 3 coatings, (d) 4 coatings, (e) 5 coatings.

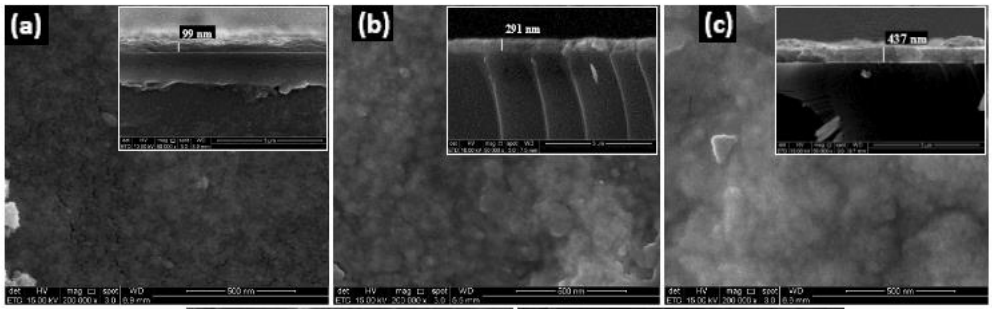

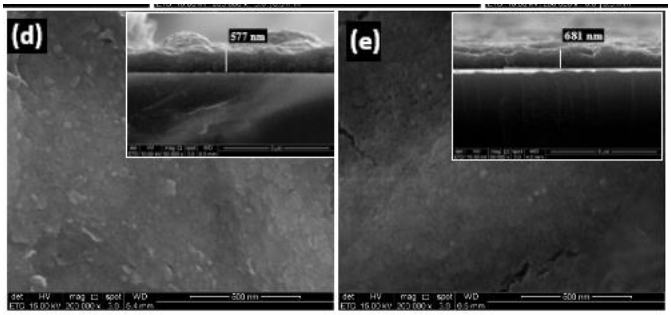

Source: self-authored

The optical properties of MZO thin films were examined as a function of film thickness using UV-visible spectroscopy with λ ranges from 350 to 800 nm (Figure 4.a). The transmittance in the visible spectrum decreases with the increasing of coating number, as shown in the inset of Figure 4.a, which illustrates the trend of average transmittance values for each layer. Additionally, all MZO thin films exhibit a blunt absorption edge that broadened with increasing thickness, accompanied by a redshift in the absorption edge.

The highest average transmittance was observed in the thinnest sample (one layer), which was below 50%. It is understood that an increase in film thickness influences light scattering, leading to a decrease in transmittance(Boukhari, Deghfel et al. 2021) .Additionally, a rise in Mn content correspondingly reduces the transmittance. Although a consistent trend in transmittance behavior is noted with respect to thickness, the average transmittance of 4% Mn-doped ZnO (MZO) thin films produced via Sol-Gel spin coating and 5% MZO thin films produced via RF magnetron sputtering was higher than that of the current study at the same thickness(Venkaiah and Singh 2014, Boukhari, Deghfel et al. 2021). This discrepancy may be attributed to differences in the deposition technique(Boukhari, Deghfel et al. 2021). However, a blunt absorption edge was observed in Figure 4.d. Increasing the thickness results in a redshift of the absorption edge. This slight shift towards longer wavelengths can be attributed to a decrease in carrier concentration due to a reduction in grain size and improved crystallinity (Bouderbala, Hamzaoui et al. 2008) .Consequently, The band gap is influenced by the grain size, strain, and point defect density, exhibiting a slight decrease from 2.85 eV to 2.10 eV with the coating number (Table 2)(Boukhari, Deghfel et al. 2021).

The absorption coefficient α, the extinction coefficient k, the refractive

index n were calculated from the transmittance and the absorbance (Mazhdi, Saydi et al. 2013, Kim and Leem 2016), and these parameters are presented for MZO thin films (Figure 4.b, c). The straight line fitting of the factors $1/(n^2-1)$ versus the squared photon energy (E^2) (DrDomenico Jr and Wemple 1969) (inset in Figure 4.c), enable us to estimate for MZO thin films, the static refractive index n_0, the dispersion energy Ed, the average oscillator energy E_o, and static dielectric constant ε_o (Table 2).

Table 2. Optical parameters of of 7%MZO thin films for various deposited layers.

Number of Layers	Dispersion energy E_d (eV)	Single-oscillator energy E_0 (eV)	Static dielectric constant ε_0 (refractive index n_0)	Urbach tail energy (eV)	Band gap energy E_g (eV)
1	10.05	5.72	1.56 (1.25)	0.63	2.86
2	7.29	5.26	1.72 (1.31)	0.64	2.63
3	3.82	4.81	2.25 (1.50)	0.97	2.40
4	2.82	4.57	2.61 (1.61)	0.97	2.28
5	2.61	4.28	2.64 (1.62)	0.85	2.14

Source: self-authored

The refractive index and the dielectric function increase with energy of the visible light and is affected by number of layer due to the increase in the crystallite size (Table 1). The absorption coefficient remains constant with increasing incident energy up to a certain point in the visible range, after which it shifts to lower energy and increases sharply with film thecknesses, indicating a decrease in E_g. These results agree with those previously reported in the literature for MZO thin films(Venkaiah and Singh 2014, Boukhari, Deghfel et al. 2021).

Figure 4. Optical transmission spectra (a), absorption coefficient (b), complex refractive index (c) and $(\alpha hv)^2$ versus photon energy hv (d) of 7% MZO samples for various coating numbers. Inset in (a) shows The average T(%) . Inset in (b) shows ln(α) versus photon energy.,Inset in (c) shows $1/(n^2-1)$ versus E^2.

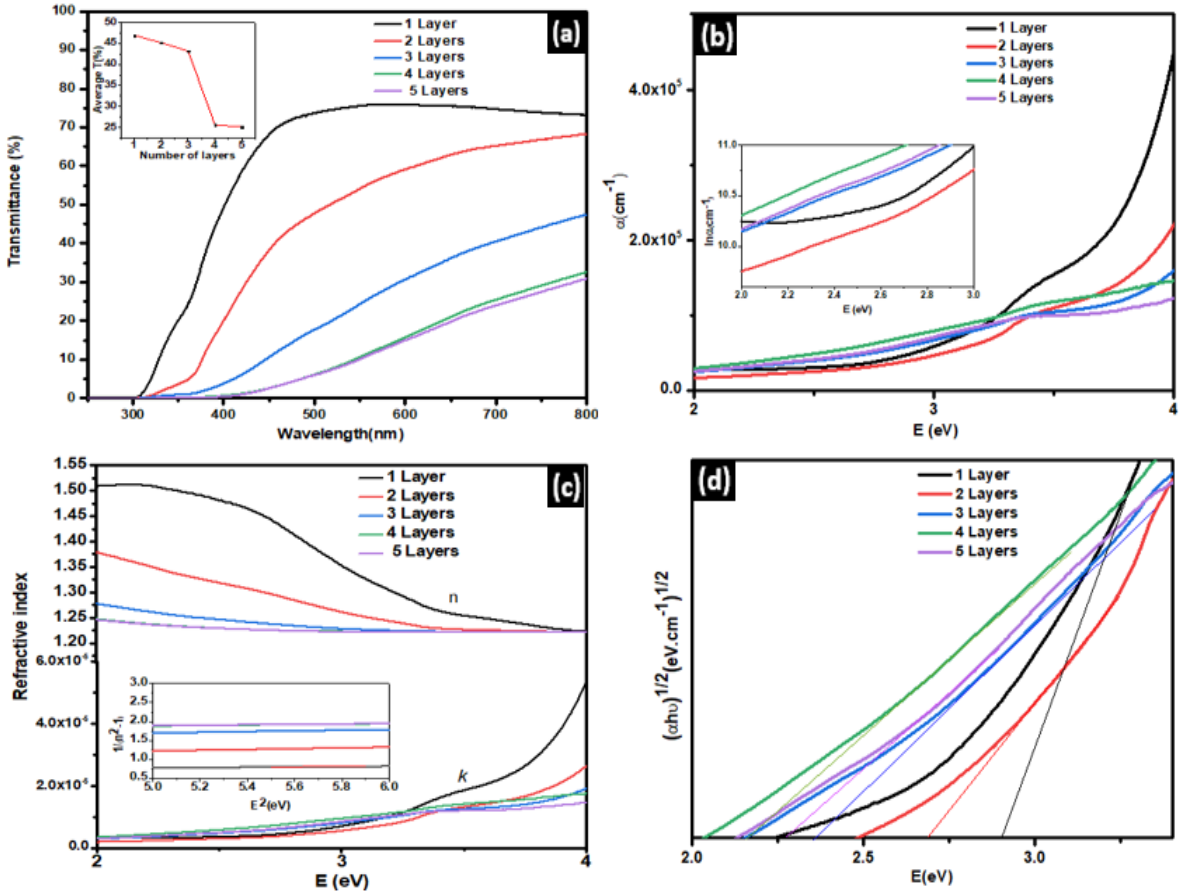

Source: self-authored

4 CONCLUSION

The effect of low thickness on the properties of MZO thin films synthesized by the spin coating method, was investigated. The main findings are as follows:

All films exhibited a polycrystalline hexagonal phase with a (002) preferential orientation. The grains, uniformly round, the lattice strain, the average crystallite size and the crystanillity were affected by increasing thickness.

The morphology showed irregularly sized aggregated clusters and the surface becomes smooth at lower thicknesses.

The band gap was found to be highly sensitive to grain size, strain, and point defect density, exhibiting a slight decrease from 2.86 eV to 2.14 eV with the increasing coating number.

As film thickness increases, transmittance decreases due to light scattering, while both the refractive index and dielectric function rise with visible light energy,

influenced by the number of layers and the corresponding increase in crystallite size.

ACKNOWLEDGEMENTS

The authors wish to thank the Algerian Ministry of Higher Education and Scientific Research represented by the Thematic Research Agency in Health and Life Sciences (TRAHLS) for financial support under the National Research Programs (NRP).

REFERENCES

Amari, R., et al. (2018). "Structural, optical and luminescence properties of ZnO thin films prepared by sol-gel spin-coating method: effect of precursor concentration." Chinese Physics Letters 35(1): 016801.

Baig, F. and G. S. Butt (2023). "Impact of copper doping on optical, UV induced wettability and photo-catalytic properties of sol-gel synthesized ZnO thin films." J Optik 288: 171196.

Bouderbala, I. Y., et al. (2024). "Optical band-diagram, Urbach energy tails associated with photoluminescence emission in defected ZnO thin films deposited by sol–gel process dip-coating: effect of precursor concentration." Applied Physics A 130(3): 205.

Bouderbala, M., et al. (2008). "Thickness dependence of structural, electrical and optical behaviour of undoped ZnO thin films." Physica B: Condensed Matter 403(18): 3326-3330.

Boukhari, A., et al. (2021). "Thickness effect on the properties of Mn-doped ZnO thin films synthesis by sol-gel and comparison to first-principles calculations." Ceramics International 47(12): 17276-17285.

Boukhari, A., et al. (2021). Thickness Effect on the Properties of 4% Mn-Doped ZnO Thin Films Grown by Sol-Gel Spin Coating Deposition. Macromolecular Symposia, Wiley Online Library

Bouznit, Y., et al. (2012). "RF magnetron sputtering of ZnO and Al-doped ZnO films from ceramic and nanopowder targets: a comparative study." Journal of Sol-Gel Science and Technology 61: 449-454.

Chen, W., et al. (2007). "Influence of doping concentration on the properties of ZnO: Mn thin films by sol–gel method." Vacuum 81(7): 894-898.

DrDomenico Jr, M. and S. J. J. o. A. P. Wemple (1969). "Oxygen-octahedra ferroelectrics. I. Theory of electro-optical and nonlinear optical effects." 40(2): 720-734.

Fabbiyola, S., et al. (2016). "Structural, microstructural, optical and magnetic properties of Mn-doped ZnO nanostructures." Journal of Molecular Structure 1109: 89-96.

Gaikwad, R. S., et al. (2014). "Effect of concentration of precursor on intrinsic ZnO thin films by spray pyrolysis." Asian Journal of Multidisciplinary Studies 2(5): 110.

Giannouli, M. and F. Spiliopoulou (2012). "Effects of the morphology of nanostructured ZnO films on the efficiency of dye-sensitized solar cells." Renewable Energy 41: 115-122.

Horcas, I., et al. (2007). "WSXM: A software for scanning probe microscopy and a tool for nanotechnology." Review of scientific instruments 78(1).

Kakati, N., et al. (2010). "Thickness dependency of sol-gel derived ZnO thin films on gas sensing behaviors." Thin Solid Films 519(1): 494-498.

Kato, H., et al. (2003). "Homoepitaxial growth of high-quality Zn-polar ZnO films by plasma-assisted molecular beam epitaxy." Japanese journal of applied physics 42(8B): L1002.

Kayani, Z. N., et al. (2015). "Structural, optical and magnetic properties of manganese zinc oxide thin films prepared by sol–gel dip coating method." Superlattices and Microstructures 82: 472-482.

Kayani, Z. N., et al. (2019). "Influence of Al percentage on the magnetic, optical, and structural properties of Al-doped CoZnO thin films." Journal of the Australian Ceramic Society 55: 479-487.

Kim, Y. and J.-Y. Leem (2016). "Effects of Precursor Concentration on Structural and Optical Properties of ZnO Thin Films Grown on Muscovite Mica Substrates by Sol–Gel Spin-Coating." Journal of nanoscience and nanotechnology 16(5): 5186-5189.

Kumar, V., et al. (2019). "Investigation of structural and optical properties of ZnO thin films of different thickness grown by pulsed laser deposition method." Physica B: Condensed Matter 552: 221-226.

Mazhdi, M., et al. (2013). "A study on optical, photoluminescence and thermoluminescence properties of ZnO and Mn doped-ZnO nanocrystalline particles." 124(20): 4128-4133.

Mortezaali, A., et al. (2016). "Thickness effect of nanostructured ZnO thin films prepared by spray method on structural, morphological and optical properties." Microelectronic Engineering 151: 19-23.

Müller, R., et al. (2019). "Chemical vapor deposition growth of zinc oxide on sapphire with methane: initial crystal formation process." J Crystal Growth and Design 19(9): 4964-4969.

Namoune, A., et al. (2017). "Thickness, annealing and substrate effects on structural, morphological, optical and waveguiding properties of RF sputtered ZnO thin films." Journal of Materials Science: Materials in Electronics 28: 12207-12219.

Pal, D., et al. (2017). "Effect of substrates and thickness on optical properties in atomic layer deposition grown ZnO thin films." Applied Surface Science 421: 341-348.

Pearton, S. and F. Ren (2014). "Advances in ZnO-based materials for light emitting diodes." Current Opinion in Chemical Engineering 3: 51-55.

Rajalakshmi, R. and S. Angappane (2014). "Effect of thickness on the structural and optical properties of sputtered ZnO and ZnO: Mn thin films." Journal of Alloys and Compounds 615: 355-362.

Rajamanickam, N., et al. (2014). "Effect of Mn-doping on the structural, morphological and optical properties of ZnO nanorods." Superlattices and Microstructures 65: 240-247.

Shishiyanu, S. T., et al. (2005). "Sensing characteristics of tin-doped ZnO thin films as NO2 gas sensor." Sensors and Actuators B: Chemical 107(1): 379-386.

Smaali, A., et al. (2020). "Pulsed laser deposited transparent and conductive V-doped ZnO thin films." J Thin Solid Films 700: 137892.

Venkaiah, M. and R. Singh (2014). "Effect of thickness on structural, optical and mechanical properties of Mn doped ZnO nanocrystalline thin films RF sputtered in nitrogen gas environment." Superlattices and Microstructures 72: 164-171.

Xin, M., et al. (2014). "Effect of Mn doping on the optical, structural and photoluminescence properties of nanostructured ZnO thin film synthesized by sol–gel technique." Superlattices and Microstructures 74: 234-241.

Yang, S. and Y. Zhang (2013). "Structural, optical and magnetic properties of Mn-doped ZnO thin films prepared by sol–gel method." Journal of Magnetism and Magnetic Materials 334: 52-58.

You, H.-C., et al. (2012). The transistor characteristics of zinc oxide active layer with different thickness of zinc oxide thin-film. 2012 International Symposium on Computer, Consumer and Control, IEEE.

Zhu, L. and W. Zeng (2017). "Room-temperature gas sensing of ZnO-based gas sensor: A review." J Sensors Actuators A: Physical 267: 242-261.